Gravity Inversion of the Basement Relief of Extensional Basins using the Total Variation Penalization Functional

Williams Almeida Lima*, João Batista Corrêa da Silva, CPGF/UFPA, Brazil and Valéria Cristina Ferreira Barbosa, ON, Brazil

This paper was prepared for presentation during the 11th International Congress of the Brazilian Geophysical Society held in Salvador, Brazil, August 24-28, 2009.

Abstract

We present a new method for the solution of the gravimetric inverse problem applied to the reconstruction of the basement relief of discontinuous sedimentary basins where the density contrast between the sediments and the basement is supposed to be known and constant or varying monotonically with depth. The solution is stabilized through the total variation (TV) functional which does not penalize solutions presenting depth discontinuities. We compare the proposed method with the global smoothness (GS), the weighted smoothness (WS) and the entropic regularization (ER) using synthetic data produced by 2D and 3D basins with discontinuous basement relief. The solution obtained with the proposed method is better than those obtained with the GS and similar to or better than those obtained with the WS and ER methods. In contrast with the WS, the TV does not require a priori information about the maximum depth of the basin. In comparison with the ER, the TV is operationally simpler and requires the specification of only one regularization parameter. The methods TV, GS, and WS where applied to the gravity anomaly above the Steptoe Valley, Nevada, USA. The TV produced a basement relief estimate presenting sharp, high-angle discontinuities. The GS failed to reproduce a solution compatible with the tectonic environment of the area and the WS produced discontinuities with unsharpened edges. Moreover, the TV when compared with the WS defined more clearly a small and shallower sub-basin in the southern extreme of the area. The methods TV and ER were applied to the 1D gravity anomaly across the Buyuk Menderes graben, west Turkey, producing overall comparable solutions. The TV, however, produces better-defined plateaus in the southern border of the graben.

Introduction

The interpretation of gravity anomalies for oil exploration in sedimentary basins consists mainly of the search for probable structural traps, like faults, through the mapping of the basement relief. The solution of this problem is unstable, reflecting the low information content in the gravity anomaly to retrieve the desired information. The usual procedure in this case is to introduce geological a priori information through the minimization of a stabilizing functional (Tikhonov and Arsenin, 1977). It is important that the geological information introduced via minimization of this functional be realistic with respect to the basement relief geometry; otherwise, the solution will be compatible with the data, will be stable, but will have no geological meaning.

In the case of structural traps generated by small flexures, as in case of intracratonic basins, the basement relief is smooth and this a priori geological information is incorporated to the problem through a functional known as global smoothness (Oldenburg, 1974; Guspí, 1990 and Barbosa et al., 1997). The minimization of this functional penalizes sharp variations in the basement relief estimate, favoring, in this way, solutions exhibiting estimated depths at neighboring points close to each other. On the other hand, in the case of extensional basins, the basement relief is shaped by normal and listric faults, presenting locally smooth plateaus, separated by sharp discontinuities. In this geological environment it is more adequate to minimize functionals that do not penalize discontinuities in the solution. Among the functionals available in the literature, the weighted smoothness (WS) and the entropic regularization (ER) are particularly suited to the interpretation of a discontinuous basement relief.

The WS (Barbosa et al., 1999) imposes that the estimated basement relief be overall smooth, allowing violation of this restriction at limited areas. This requirement introduces a certain level of instability in the solution, making it necessary to introduce a priori information about the basement maximum depth.

The ER (Campos Velho and Ramos, 1997; Ramos et al., 1999; Silva et al., 2007) consists in minimizing the first-order entropy of the solution, which favors estimated solutions presenting discontinuities with large vertical slips, in contrast with the GS which penalizes such discontinuities. The minimization of the first-order entropy incorporates a priori information similar to that introduced in the WS, differing from it by requiring no a priori information about the maximum depth of the basement. This feature makes the ER a more robust method than the WS, requiring less a priori geological information to stabilize the solutions. On the other hand, the minimization of the first-order entropy tends to minimize also the zero-order entropy, favoring, in this way, solutions with a minimum number of discontinuities presenting very high and unrealistic slips. These solutions are not geologically feasible and are avoided with the "maximization" of the zero-order entropy. This "maximization", in fact, avoids the excessive minimization of the zero-order entropy. The combination of the minimization of the first-order entropy with the maximization of the zero-order entropy requires the specification of two regularizing parameters, leading to an enormous operational difficulty.

We present a new gravity inversion method applied to the mapping of the discontinuous basement relief of sedimentary basins. The stabilizing functional is the total variation (Rudin et al., 1992; Acar and Vogel, 1994), that consists in minimizing the L_1-norm of the spatial derivative of the function representing the basement relief. This functional does not penalize sharp variations in the solution, requires no extra a priori information as is the case of the WS, and, in contrast with the ER, requires the specification of only one regularization parameter.

The application of the method on 1D and 2D synthetic data showed that it produces results similar to or better than the results obtained with the WS and ER methods. The proposed method was also applied to the Bouguer gravity anomaly of the northern portion of the Steptoe Valley, Nevada, USA, in the Great Basin province. This anomaly consists of gravity lows due to the presence of down thrown crustal blocks with large vertical displacements (Carlson and Mabey, 1963). The results were compared with those produced by the GS and WS, and showed a topography exhibiting not only sharper discontinuities, but also a better definition of a sub-basin at the southern portion of the studied area.

Method

Let $\mathbf{g^o}$ be an *N*-dimensional vector of gravity observations. These observations are assumed to be produced by a sedimentary basin where the density contrast between the sediments and the basement is known and constant or varying with depth. We want to estimate the basement relief, *S*, (Figures 1a and 1b) using as interpretation model a set of *M* 2D or 3D vertical juxtaposed prisms, along, respectively, the *x*-direction (Figure 1a) or the *x*-and *y*-directions (Figure 1b). The thicknesses, p_j, of the prisms are the parameters to be estimated (Figures 1a and 1b). The top of each prism coincides with the earth's surface and all prisms have the same horizontal dimension.

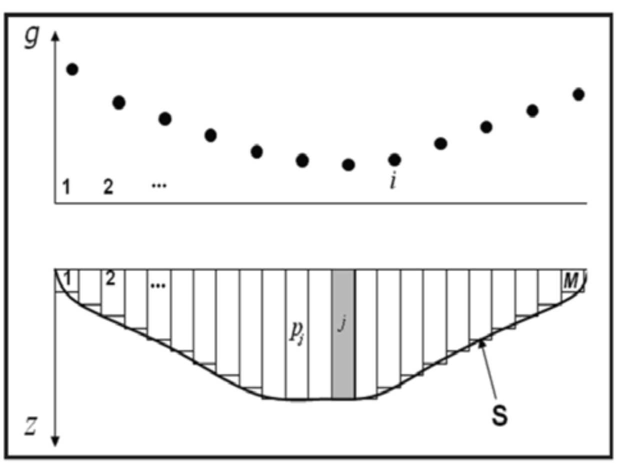

Figure 1a –Interpretation model for the case of 2D basins.

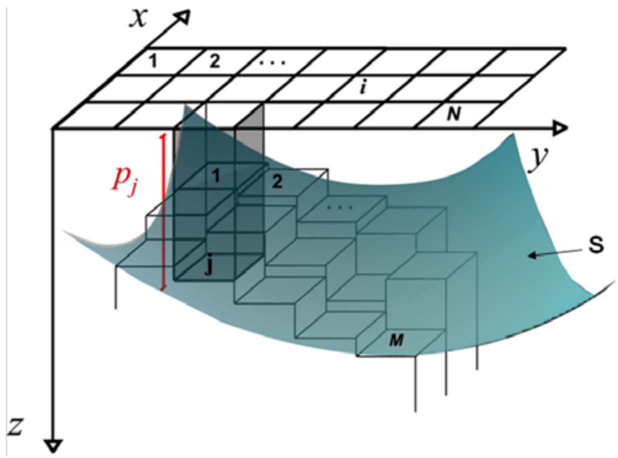

Figure 1b – Interpretation model for the case of 3D basins.

The gravity inversion consists in the estimation of vector $\mathbf{p} = [p_1, \cdots, p_M]^T$, given the vector $\mathbf{g}^0(\mathbf{p}) \equiv [g_1^0, \cdots, g_N^0]^T$ containing *N* observations of the gravity anomaly. The fitting of the gravity data is imposed by the minimization, with respect to **p**, of the nonlinear functional $\|\mathbf{g}^o - \mathbf{g}(\mathbf{p})\|^2$, where $\mathbf{g}(\mathbf{p})$ is an *N*-dimensional vector containing the computed anomaly, using the interpretation model, at the same observation points, and $\|\cdot\|$ is the Euclidean norm. The *i*th element $g_i(\mathbf{p})$ is the gravity anomaly produced by the *M* prisms at the *i*th observation point. This is an ill-posed inverse problem characterized by unstable solutions. Thus, in order to stabilize it, one must introduce additional a priori information, which can be accomplished by classical regularization techniques such as the GS, where the solution is constrained to be smooth. In this case, the estimate $\hat{p}_i$ (thickness of the *i*th prism) must be close to the estimate $\hat{p}_j$ (thickness of the *j*th prism, adjacent to the *i*th prism), subject to fitting the data within the experimental precision. In the case of 2D basins, this proximity condition is imposed along the *x*-direction, whereas, in 3D basins, it is imposed along the *x*- and *y*-directions. Mathematically, this condition is imposed through the minimization of the functional $\rho(\mathbf{p}) = \|\mathbf{g}^o - \mathbf{g}(\mathbf{p})\|_2^2 + \mu\|\mathbf{Rp}\|_2^2$, where μ is the smallest positive value capable of producing stable solutions, and **R** is a matrix whose rows have only two non zero elements equal to 1 and –1, localized at the columns corresponding to parameters *i* and *j*, whose estimates must be as close to each other as possible.

The WS method, developed by Barbosa et al. (1999), is specially designed to the interpretation of a discontinuous basement relief of a sedimentary basin. This method minimizes the functional

$$\sigma(\mathbf{p}) = \|\mathbf{g}^o - \mathbf{g}(\mathbf{p})\|^2 + \mu_s\|\mathbf{WRp}\|^2 + \mu_r\|\mathbf{p} - \mathbf{p}_{\max}\|^2,$$

where μ_s is the smallest positive value that, combined with the largest positive value of μ_r produce stable solutions with a number of discontinuities compatible with the a priori geological information available, $\boldsymbol{W}$ is a diagonal weighting matrix and $\mathbf{p}_{max}$ is an M-dimensional vector of maximum depths of the basement relief, known a priori. The diagonal element w_{kk} of matrix $\boldsymbol{W}$ assigns smaller weights to the constraint imposing proximity between the kth pair of adjacent prisms thickness estimates, $\hat{p}_i$ and $\hat{p}_j$, which are associated with regions of sharp discontinuities in the basement relief. Matrix $\boldsymbol{W}$ is defined iteratively and automatically, being initialized with the identity matrix.

Silva et al. (2007) applied the ER (Campos Velho and Ramos, 1997; Ramos et al., 1999) to gravimetric data generated by 2D sedimentary basins, where the basement presents sharp discontinuities. The ER consists in the minimization of the first-order entropy of the parameters estimates:

$$Q_1(\mathbf{p}) = -\sum_{k=1}^{L} S_k \log(S_k), \tag{1}$$

with

$S_k = |r_k| \Big/ \sum_{i=1}^{L} |r_i|$ and $r_k = |\hat{p}_i - \hat{p}_j| + \varepsilon$, subject to the fit of the geophysical data within the expected noise level, with $\hat{p}_i$ and $\hat{p}_j$ being depth estimates of adjacent prisms, and L the number of such pairs. The physical meaning of the minimization of the entropy is displayed in Figure 2. According to Silva et al. (2007) the minimization of $Q_1(\mathbf{p})$ implies on the minimization of the number of discontinuities in the estimates of the prisms thicknesses used to define the interpretation model. The global smoothness constraint produces estimates similar to the basin B1 (Figure 2a), whereas the minimization of $Q_1(\mathbf{p})$ favors estimates similar to basins B2 and B3 (Figures 2b and 2c). Figure 2d shows the values of $Q_1(\mathbf{p})$ associated to the basins B1-B3 as well as the values of the zero-order entropy, $Q_0(\mathbf{p})$, defined by the equation (1) with $S_k = |r_k| \Big/ \sum_{i=1}^{M} |r_i|$ and $r_k = |\hat{p}_i| + \varepsilon$. Note that a small decrease in $Q_1(\mathbf{p})$ (between B2 and B3 in Figure 2d) corresponds to a great decrease in $Q_0(\mathbf{p})$. In the gravimetric interpretation of extensional basins, we are interested in basins of type B2 because narrow basins like B3 are not geologically meaningful. Thus, it is necessary to avoid the excessive minimization of $Q_0(\mathbf{p})$, and this is accomplished, algorithmically, through its "maximization". In this way, the ER consists of the minimization of the functional $\tau(\mathbf{p}) = \|\mathbf{g^0} - \mathbf{g}(\mathbf{p})\|^2 - \gamma_0 Q_0(\mathbf{p}) + \gamma_1 Q_1(\mathbf{p})$, where γ_0 and γ_1 are real positive numbers chosen on the basis of the following criteria. The value of γ_1, similarly to value of μ_r, must be the largest positive value producing stable solutions and leading to a number of discontinuities in accordance with the geological knowledge about the basin's basement. The parameter γ_0, is initially assigned a very small value (including zero). If the estimated basin geometry presents horizontal dimensions substantially smaller than the expected ones, on the basis of a priori geological knowledge, the value assigned to γ_0 must be increased.

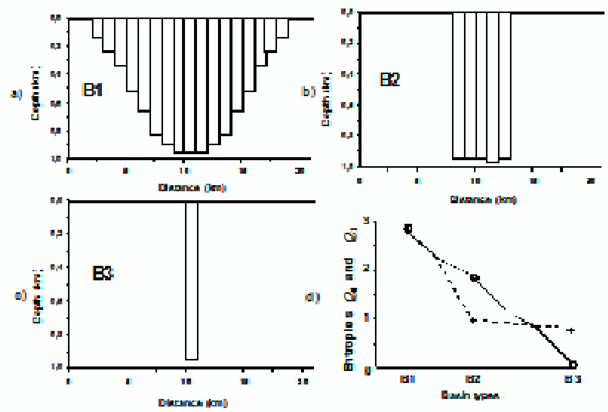

Figure 2 – (a)-(c) Basin types. (d) Corresponding values of de $Q_0(\mathbf{p})$ (continuous line) and $Q_1(\mathbf{p})$ (dashed line) associated to each kind of basin.

The total variation method (TV) consists in the minimization of the functional $\varphi(\mathbf{p}) = \|\mathbf{g}^0 - \mathbf{g}(\mathbf{p})\|^2 + \alpha \sum_{1}^{K} \sqrt{|p_i - p_j|^2 + \beta}$, where p_i and p_j are the thicknesses of two adjacent prisms, K is the number of pairs of such prisms, α and β are non negative scalars, β being always a small value (typically in the order of 10^{-4}), introduced to avoid numerical singularities. Parameter α controls the overall stability and the degree of discontinuities present in the solution. The larger the value of α, the more stable is the solution and the larger is the number of discontinuities.

The above methods were formulated as nonlinear optimization problems and solved iteratively. The GS and the WS were implemented using Newton's method while the ER and the TV were implemented using the quasi-Newton method. In all cases, the modification proposed by Marquardt (1963) was incorporated to guarantee convergence of the iterative process. The iteration for the TV method is stopped either when the maximum number of iterations is attained or when the value of the objective function remains below a threshold, established by the interpreter, for five consecutive iterations.

Results of numerical simulations

2D Basin

Figure 3a shows in red dots the gravity observations generated by a 2D simulated graben, whose basement relief is, in general smooth, but presents, locally, sharp discontinuities (red line in Figure 3b). The density contrast between the sediments and the basement is -0.3 g/cm^3.

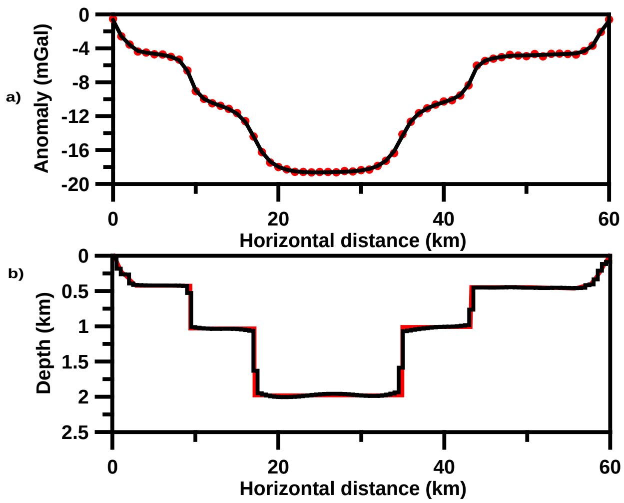

Figure 3 – Simulated Graben. (a) Observed Bouguer anomaly (red dots) and fitted anomaly using the TV (solid black line). (b) True solution (red) and estimated basin relief using the TV (black line).

Pseudorandom, Gaussian noise with zero mean and standard deviation equal to 0.1 mGal was added to the theoretical gravity anomaly. The interpretation model consists of 60 elementary prisms with density contrast of -0.3 g/cm^3. The solution produced by the TV with α = 20 and β = 0.001 (black line in Figure 3b) delineated with excellent precision the topography of the basement, in particular, its discontinuities. Figure 3a shows, in black line, the fitted gravity anomaly.

3D basin

Figures 5a and 5c show, respectively, in black contour lines and in perspective, a gravity anomaly generated by a simulated 3D basin, whose basement is characterized by step faults (Figure 5b). The density contrast between the sediments and the basement is -0.2 g/cm^3. The theoretical gravity observations were contaminated with pseudorandom Gaussian noise with zero mean and standard deviation equal to 0.1 mGal. The interpretation model consist of a grid of 25 $\times$ 25 prisms with dimensions of 2 km in the x- and y- directions, with density contrasts equal to -0.2 g/cm^3. The solution obtained by the TV method with α =1 and β= 0.001 (Figure 5d) reproduced with excellent precision the plateaus that define the topography of the basement, as well as the discontinuities separating them. Figure 5a shows, in red lines, the fitted gravity anomaly. For comparison, we show in Figures 5e and 5f the inversions of the same anomaly shown in Figures 5a and 5c employing, respectively, the GS and WS and the same interpretation model. The regularization parameters are: μ = 1.0 in the case of GS, and μ_s = 0.005, μ_r = 0.01, and a priori maximum depth of 4 km in the case of WS. The fitted anomalies (not shown) explain the observations within the experimental precision. The GS estimate (Figure 5e), as expected, produced an inferior result as compared with the one obtained with the WS (Figure 5f) and the TV (Figure 5d), not delineating the discontinuities of the basement relief.

The solutions of the WS and the TV, successfully delineated the basement relief with comparable precisions. The TV, however, estimates flatter plateaus as compared with the WS. Moreover, differently from the WS, the TV does not required a priori knowledge about the maximum basement depth.

Aplications to real data

Buyuk Menderes

Figure 4a shows in red dots the Bouguer anomaly of a gravity profile across the Buyuk Menderes valley (in West Turkey). The interpretation model consisted of 90 prisms with density contrasts varying with depth given by the hyperbolic law (Litinsky, 1989)

$$\Delta\rho(z) = \frac{\Delta\rho_0 \beta^2}{(\beta + z)^2} \ .$$

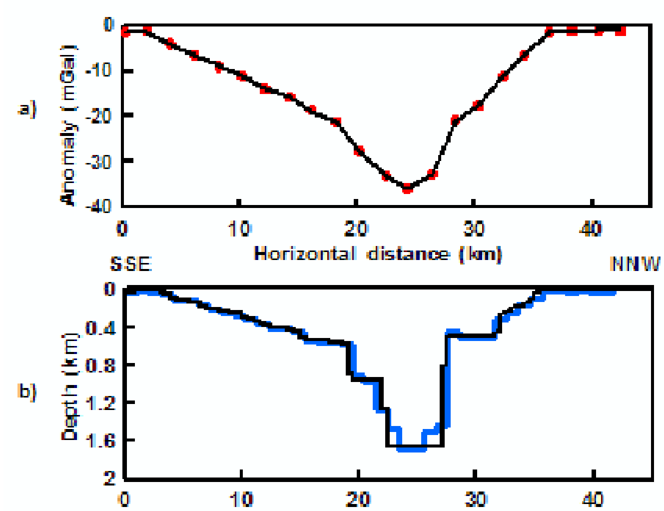

Figure 4 – Buyuk Menderes. (a) Observed bouguer anomaly (red dots) and fitted anomaly using the TV (solid black line). (b) Estimated basin relief using the TV (black) and ER (blue).

with $\Delta\rho_0 = -0.98\,\mathrm{g/cm^3}$ and $\beta = 2.597\,\mathrm{km}$ (Sari and Salk, 2002). The result of the inversion with the TV and ER are shown in Figure 4b, in black and solid blue lines respectively. We note two main differences between these solutions: *i*) the TV estimates a plane topography in the deepest part of the basement whereas the ER produces a curved one; *ii*) the topography estimated with the TV shows a better defined plateau on the SSE side, located about 20 km in the horizontal distance and depth equal to 0.9 km.

Steptoe valley

The Bouguer anomaly from the Steptoe Valley (Carlson and Mabey, 1963), corrected for deep crustal effects is shown in black contour lines in Figure 6a and in perspective in Figure 6b. The Steptoe Valley is located in the *Basin and Range* province, Nevada, USA, where the topography is dominated by the alternation of linear mountain chains and elongated valleys. This topography is the result of down throw and uplift of large crustal blocks caused by the action of large extensional forces associated to the presence of intra-plate tectonic forces. The interpretation model is composed of a grid of 42×26 prisms with dimensions of 1.25 km in the x– (N-S) and y– (E-W) directions, with density contrast of –0.3 g/cm^3. Figure 6c shows the solution stabilized by the TV method with α = 1.25 and β = 0.001. Figures 6d and 6e show, respectively, the estimates produced by the GS with μ = 1.5 and by the WS with μ_s = 0.05, μ_r = 0.001, and a priori maximum depth of 3 km. The solution stabilized by the TV (Figure 6c) exhibit a very abrupt topography with well-defined discontinuities at the borders not only of the main basin, but also of the southern sub-basin, in agreement with the tectonics of extensional forces, dominant in the *Basin and Range* province. Figure 6a shows, in red contour curves, the corresponding fitted anomaly. The GS, as expected, produced a smooth topography (Figure 6d), with rounded edges, without evidences of discontinuities produced by gravity faults. The topography estimated by the WS (Figure 6e) shows several discontinuities typical of gravity faults, but with smaller slips than that ones produced by the TV. Moreover, the southern sub-basin is not so well defined in its edges due to the borders with less accentuated inclinations, and to the uneven bottom. The fitted data produced by the GS and WS (not shown) explain the observations within the experimental precision.

Conclusions

We presented a gravimetric inversion method for mapping the discontinuous basement relief of a sedimentary basin. The solution is stabilized with the minimization of the total variation (TV) of the solution vector. The solutions obtained with this method produced much better estimates of the basement relief (including its discontinuities) than the solutions obtained with the GS method. When compared with the WS and ER methods, the TV method shows similar solutions. However, it has the advantage of neither requiring a priori knowledge about the maximum basin depth (as is the case of the WS), nor the specification of two regularization parameters (as is the case of the ER). As a result the proposed method is operationally simpler and has a great potential in producing meaningful mappings of normal faults associated with petroleum trapping.

Acknowledgments

References

Acar, R., and Vogel, C. R., 1994, Analysis of total variation penalty methods: Inverse Problems, **10**, 1217–1229.

Barbosa, V. C. F., Silva, J. B. C,and Medeiros, W. E., 1997, Gravity inversion of basement relief using approximate equality constraints on depths: Geophysics, **62**, 1745-1757.

Barbosa, V. C. F., Silva, J. B. C, and Medeiros, W. E., 1999, Gravity inversion of a discontinuous relief stabilized by weighted smoothness constraints on depth: Geophysics, **64**, p. 1429-1438.

Carlson J. E., and Mabey, D. R., 1963, Gravity and aeromagnetic map of the Ely area, White Pine County, Nevada: U.S Geol. Surv., map GP-392.

Campos Velho, H. F. and Ramos, F. M., 1997, Numerical inversion of two-dimensional geoelectric conductivity distributions from electromagnetic ground data: Revista Brasileira de Geofísica, **15**, 133-144.

Guspi, F., 1990, General 2D gravity inversion with density contrast varying with depth: Geoexploration, **26**, 253-265.

Litinsky, V.A., 1989, Concept of effective density: Key to gravity determinations for sedimentary basins. Geophysics, v.54, n.11, 1474-1482.

Marquardt, D. W., 1963, An algorithm for least-squares estimation of nonlinear parameters: J. Soc. of Ind. and Applied Math., **2**, 601-612.

Oldenburg, D. W., 1974, The inversion and interpretation of gravity anomalies: Geophysics, **39**, 526-536.

Oliveira, A. S., 2007, Inversão gravimétrica do relevo do embasamento usando regularização entrópica: Dissertação de Mestrado, UFPA.

Ramos, F. M., Campos Velho, H. F., Carvalho, J. C. and Ferreira, N. J., 1999, Novel Approaches on Entropic Regularization: Inverse Problems, **15**, 1139 – 1148.

Rudin, L.I., Osher, S. and Fatemi, E., 1992. Nonlinear total variation based noise removal algorithms, *Physica D,* **60,** 259–268.

Sari, C., Salk, M. Analysis of gravity anomalies with hyperbolic density contrast: an application to the gravity data of Western Anatolia. Journal of the Balkan Geophysical Society, v. 5, n. 3, p.87-96. 2002.

Silva, J. B. C., Oliveira, A. S. and Barbosa, V. C. F., 2007, **I**nversão gravimétrica do relevo do embasamento usando regularização entrópica: X Congresso Brasileiro de Geofísica.

Tikhonov, A. N. and Arsenin, V. Y., 1977, Solutions of ill-posed problems: V. H. Winston & Sons.

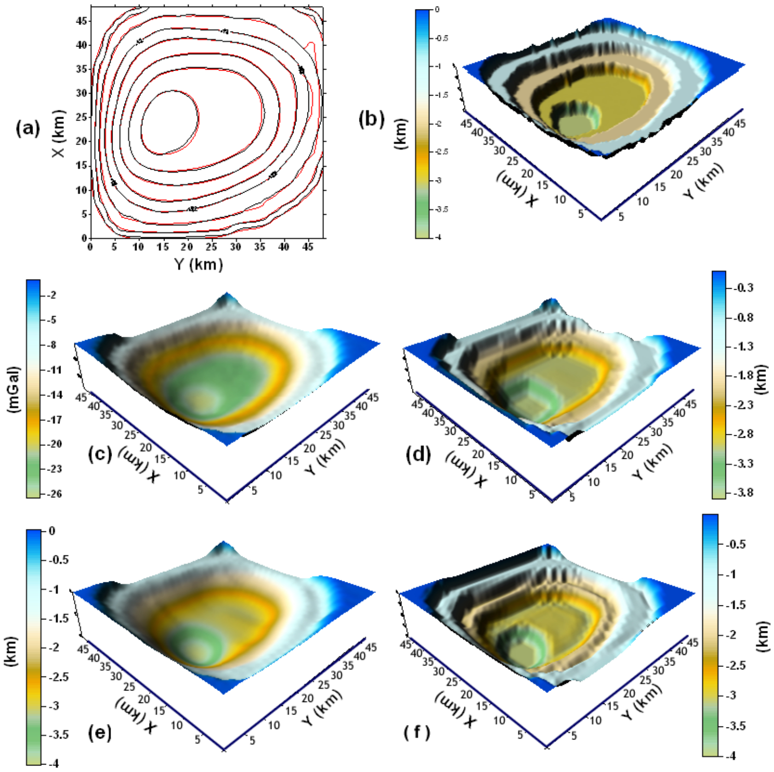

Figure 5 – Test on synthetic data. 3D Basin. (a) Gravity anomalies: observed (black lines) and fitted by the TV (red lines). (b) True model. (c) Perspective view of the gravity anomaly. (d) TV result. (e) GS result. (f) WS result.

Figure 6 – Steptoe Valley (a) Bouguer anomaly (black lines) and fitted anomaly by TV (red lines). (b) Perspective view of the Bouguer anomaly. (c) TV result. (d) GS result. (e) WS result.